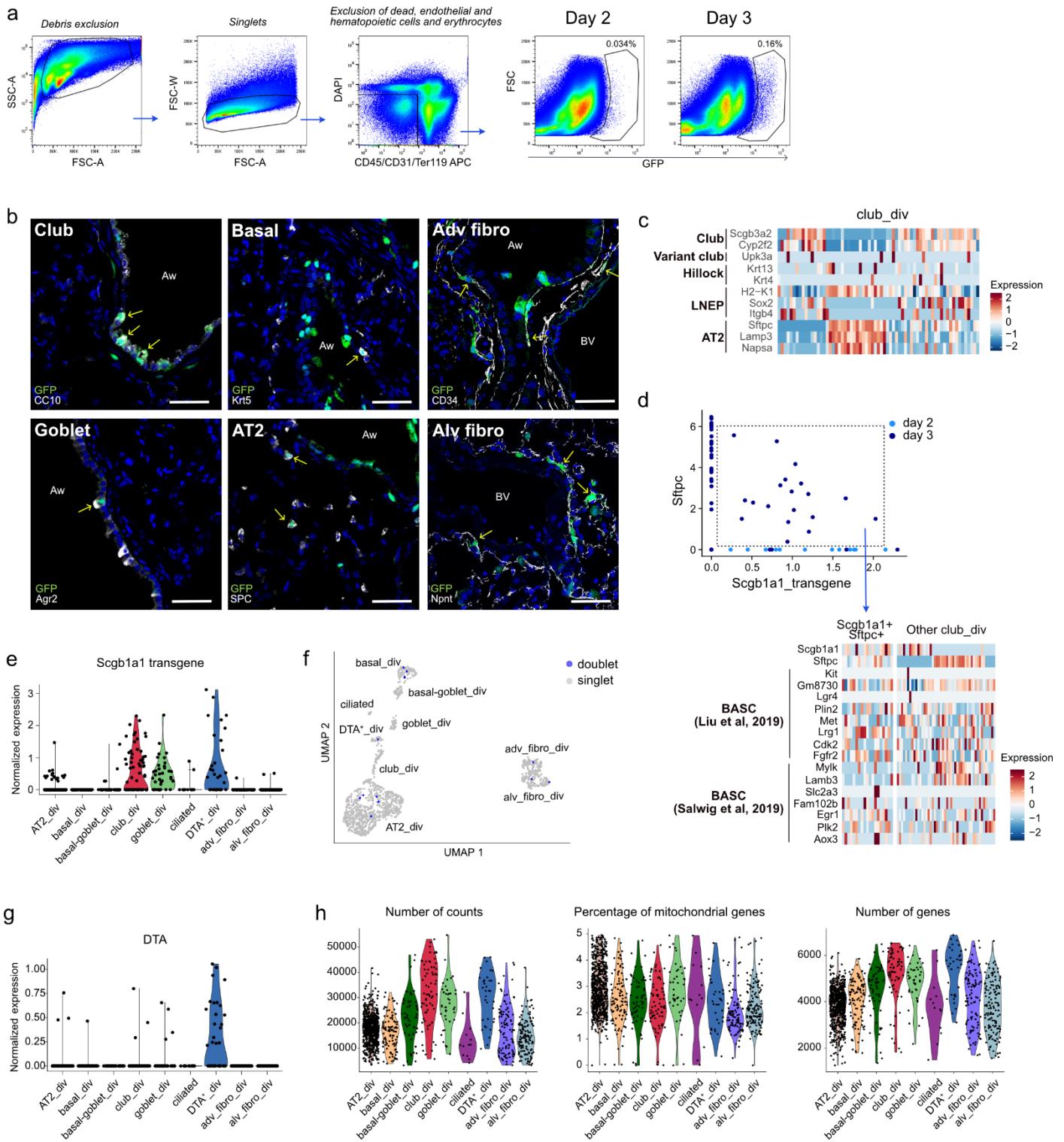


**Single-cell division tracing and transcriptomics reveal cell types
and differentiation paths in the regenerating lung**

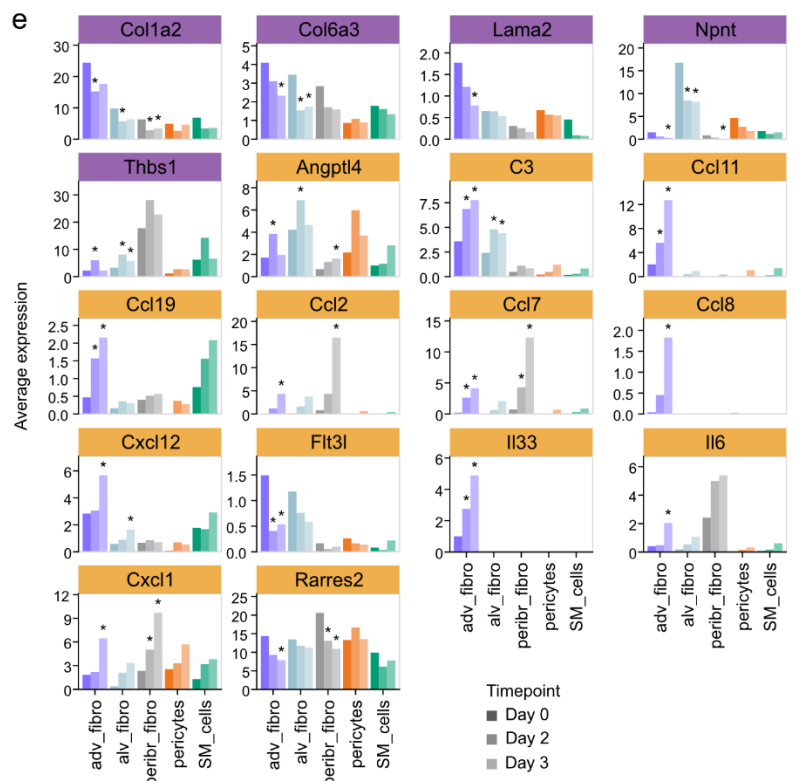
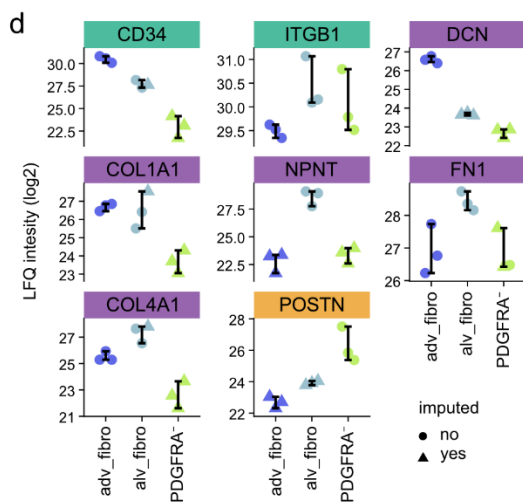
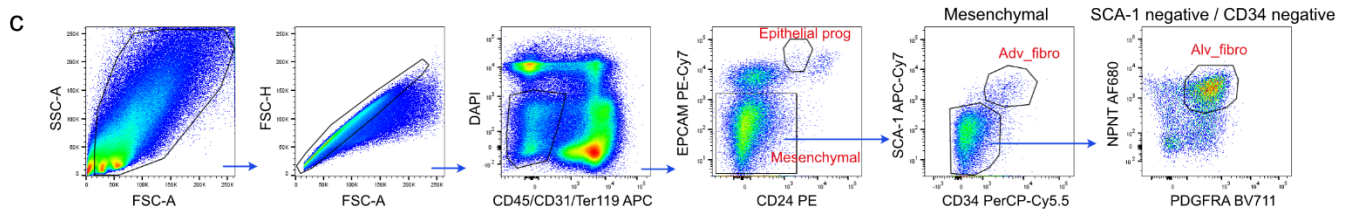
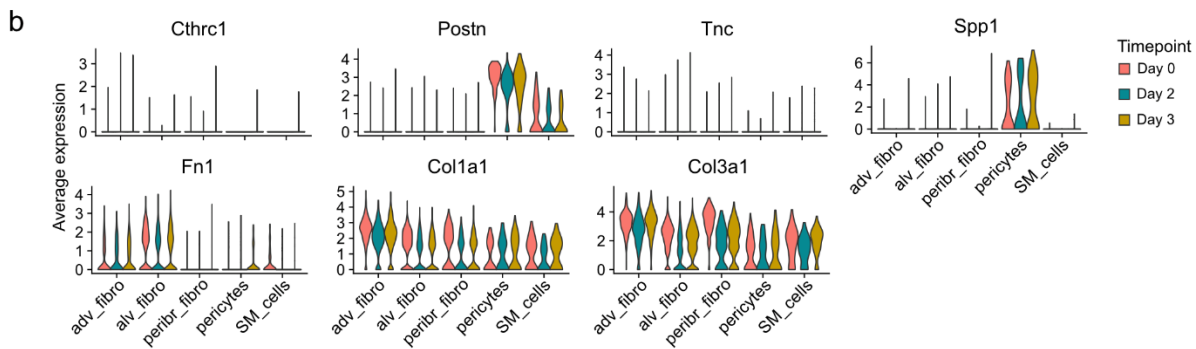
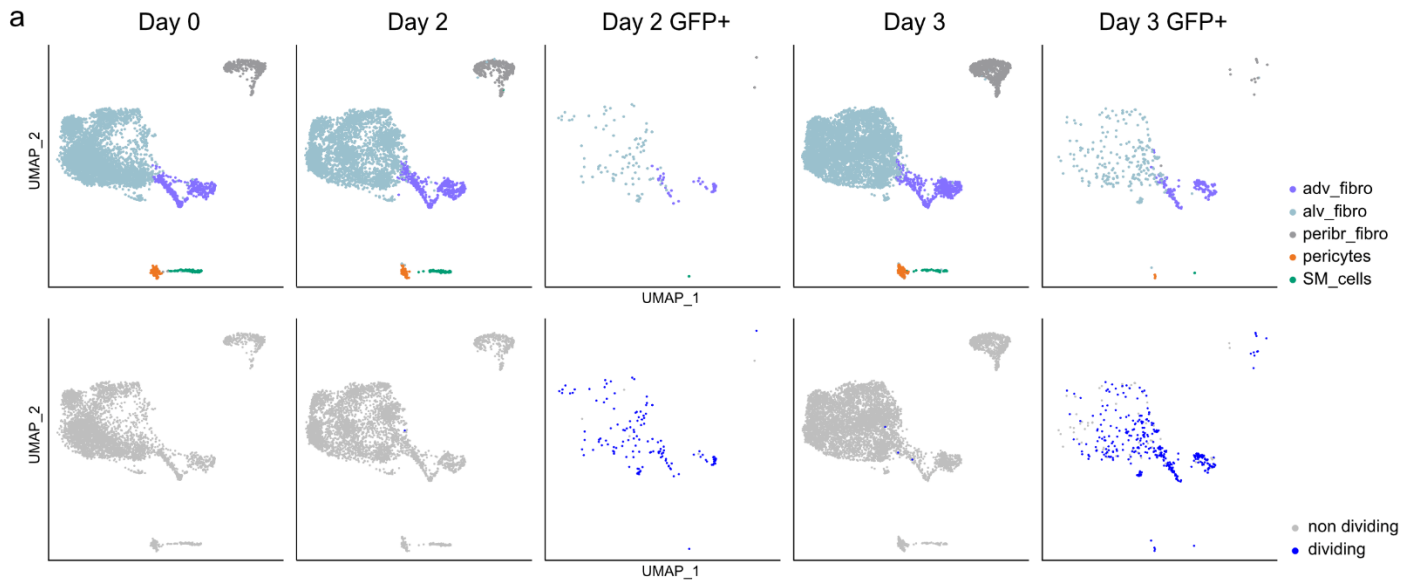
Leila R. Martins, Lina Sieverling, Michelle Michelhans, Chiara Schiller, Cihan Erkut,
Thomas G. P. Grünewald, Sergio Triana, Stefan Fröhling, Lars Velten, Hanno Glimm,
Claudia Scholl

SUPPLEMENTARY INFORMATION



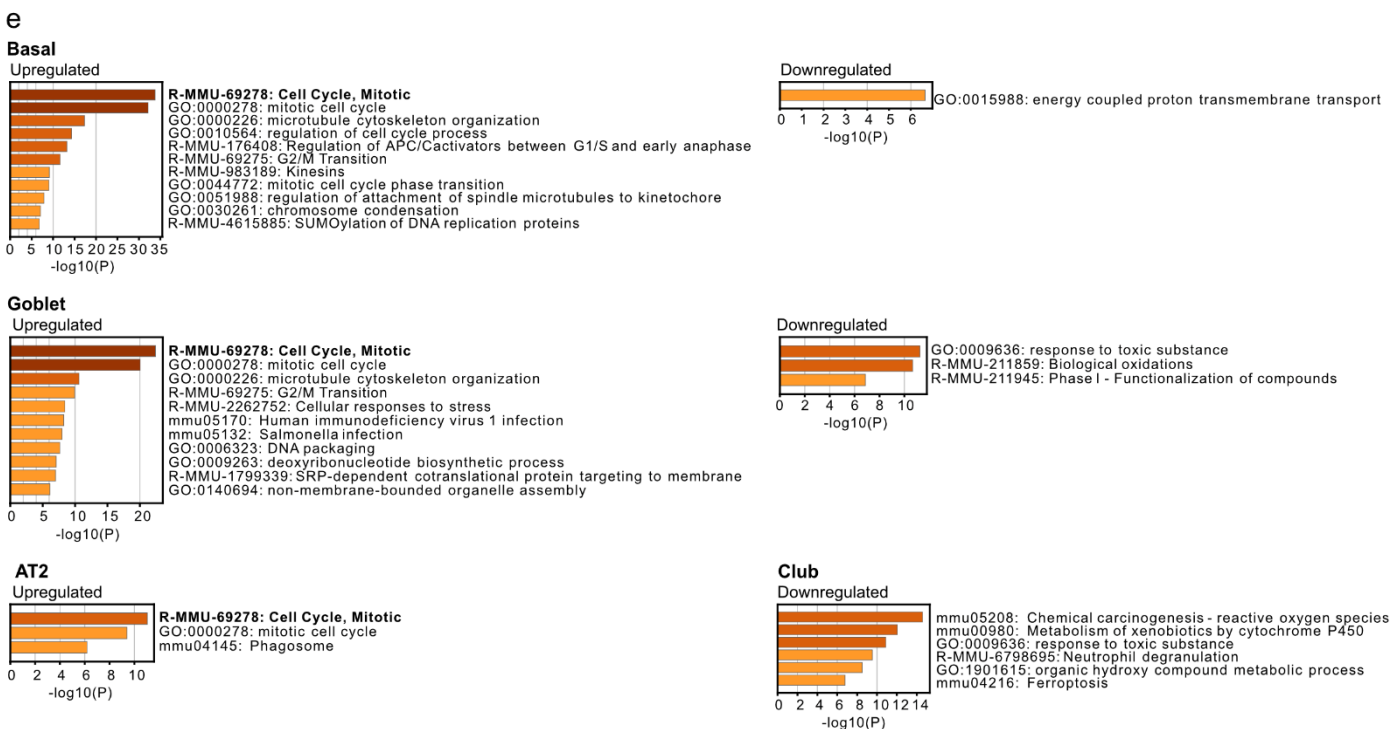
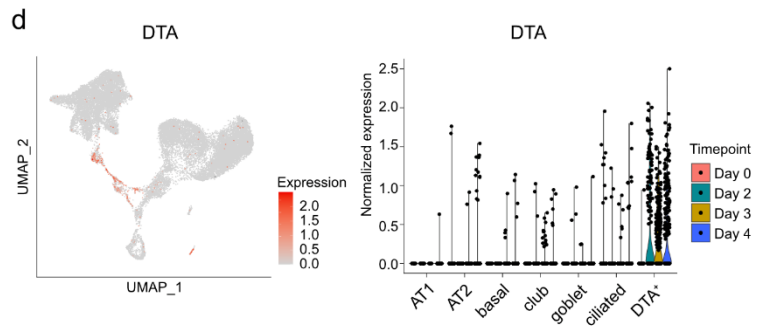
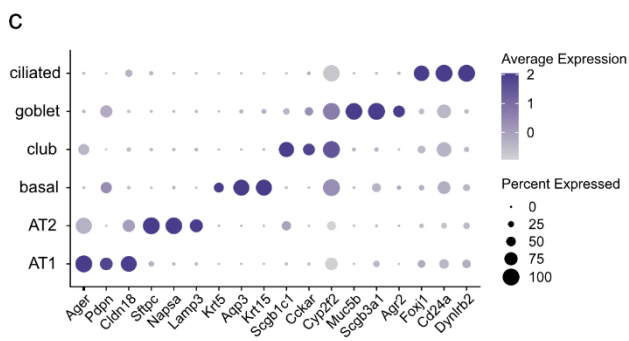
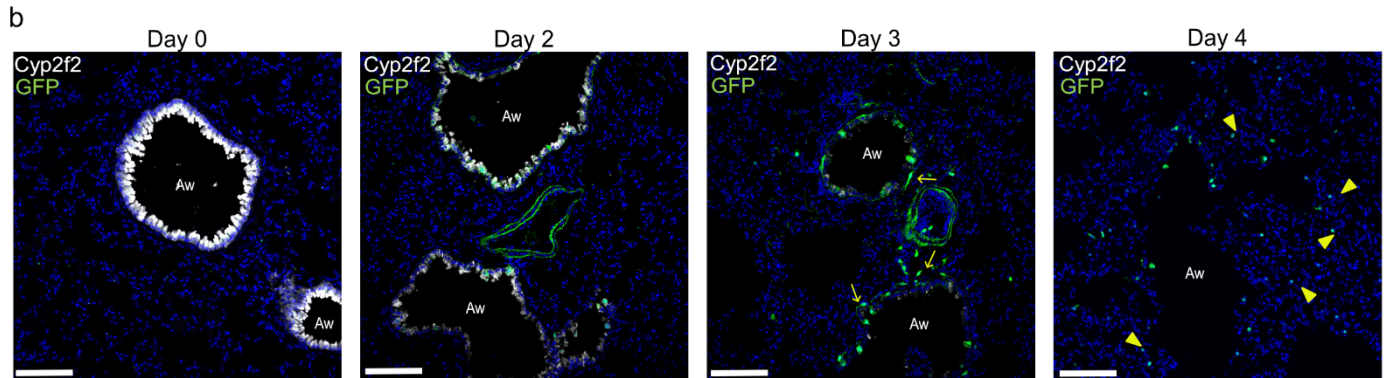
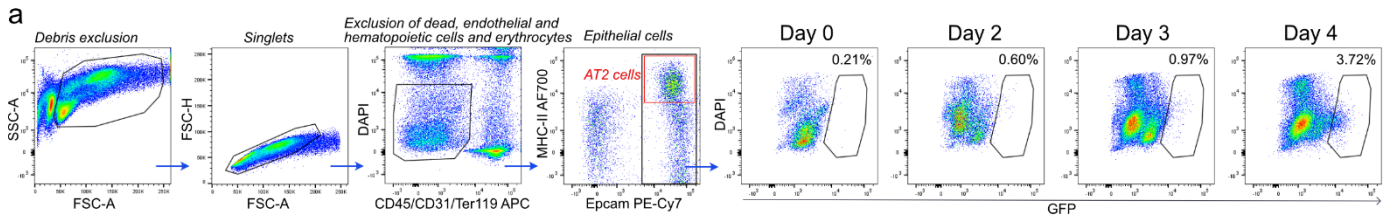
Supplementary Figure 1. Characterization of dividing cells after targeted depletion of *Scgb1a1*⁺ cells.

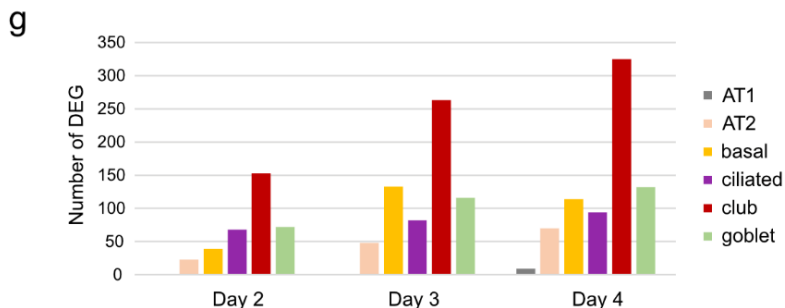
a. Gating strategy used to sort viable GFP⁺ cells. **b.** IF staining of dividing GFP⁺ cells (green) combined with markers for club cells (CC10, white), goblet cells (Agr2, white), basal cells (Krt5, white), AT2 cells (SPC, white), adventitial fibroblasts (adv fibro, CD34, white), and alveolar fibroblasts (alv fibro, Npnt, white). Nuclei are stained with DAPI (blue). All images were taken at day 3 after tamoxifen injection. Aw: airway; BV: blood vessel. Arrows are pointing to GFP⁺ cells co-stained with cell type specific markers. Representative images of more than three independent experiments with similar results are shown. Scale bar: 50 μ m. **c.** Heatmap of the main marker genes for previously described progenitor club cell types, club cells, and AT2 cells in club_div cells at day 2 and 3. **d.** Upper panel: Co-expression of the *Scgb1a1* transgene and *Sftpc* in club_div cells. Lower panel: Expression of bronchioalveolar stem cell (BASC) marker genes in club_div cells co-expressing the *Scgb1a1* transgene and *Sftpc* and in other club_div cells. **e.** Violin plot showing the expression of the *Scgb1a1* transgene in the indicated cell types. **f.** UMAP embedding showing doublet and singlet classification by scDoublet. **g.** Violin plot showing the expression of DTA in the dividing populations at day 2 and 3. **h.** Violin plots showing number of counts, percentage of mitochondrial genes, and number of genes per cell in the different dividing cell populations. The labeling of the y-axis is given in the heading.



Supplementary Figure 2. Characterization of mesenchymal cell activation after epithelial injury in SRC mice.

a. UMAP embedding of mesenchymal cells and dividing GFP⁺ mesenchymal cells on the indicated days. **b.** Violin plots showing the expression of fibrosis-associated genes in individual cells of the different mesenchymal populations on day 0, 2, and 3. **c.** Gating strategy used to sort epithelial progenitor cells (epithelial prog), adventitial fibroblasts (adv_fibro), and alveolar fibroblasts (alv_fibro). **d.** Protein expression in log₂ label-free quantification (LFQ) intensity of upregulated ligands in adventitial fibroblasts, alveolar fibroblasts, and PDGFRA negative cells (see Fig. 2f) at day 0 for which protein data were available. Three independent experiments are shown. Error bars denote standard deviation. **e.** Average normalized RNA expression of all ligands in the modified CellChat ligand-receptor database that are differentially expressed between day 0 and day 2 or day 3 in adv_fibro by scRNA-seq. *Bmp4*, *Tgfb3*, and *Mif* (included in Fig. 2g) were excluded from this figure. Asterisks denote significant differential expression on day 2 or 3 compared to day 0 (MAST test, FC \geq 1.5, p_{adj} \leq 0.05). **d, e.** Ligand genes are sorted by the possible type of interaction (yellow: secreted signaling, purple: ECM receptor, green: cell-cell contact). **a, b, e.** scRNA-seq analysis was done using total mesenchymal cells on day 0 (n=2 mice), day 2 (n=3 mice), and day 3 (n=3 mice), and GFP⁺ mesenchymal cells on day 2 (n=12 mice) and day 3 (n=3 mice).

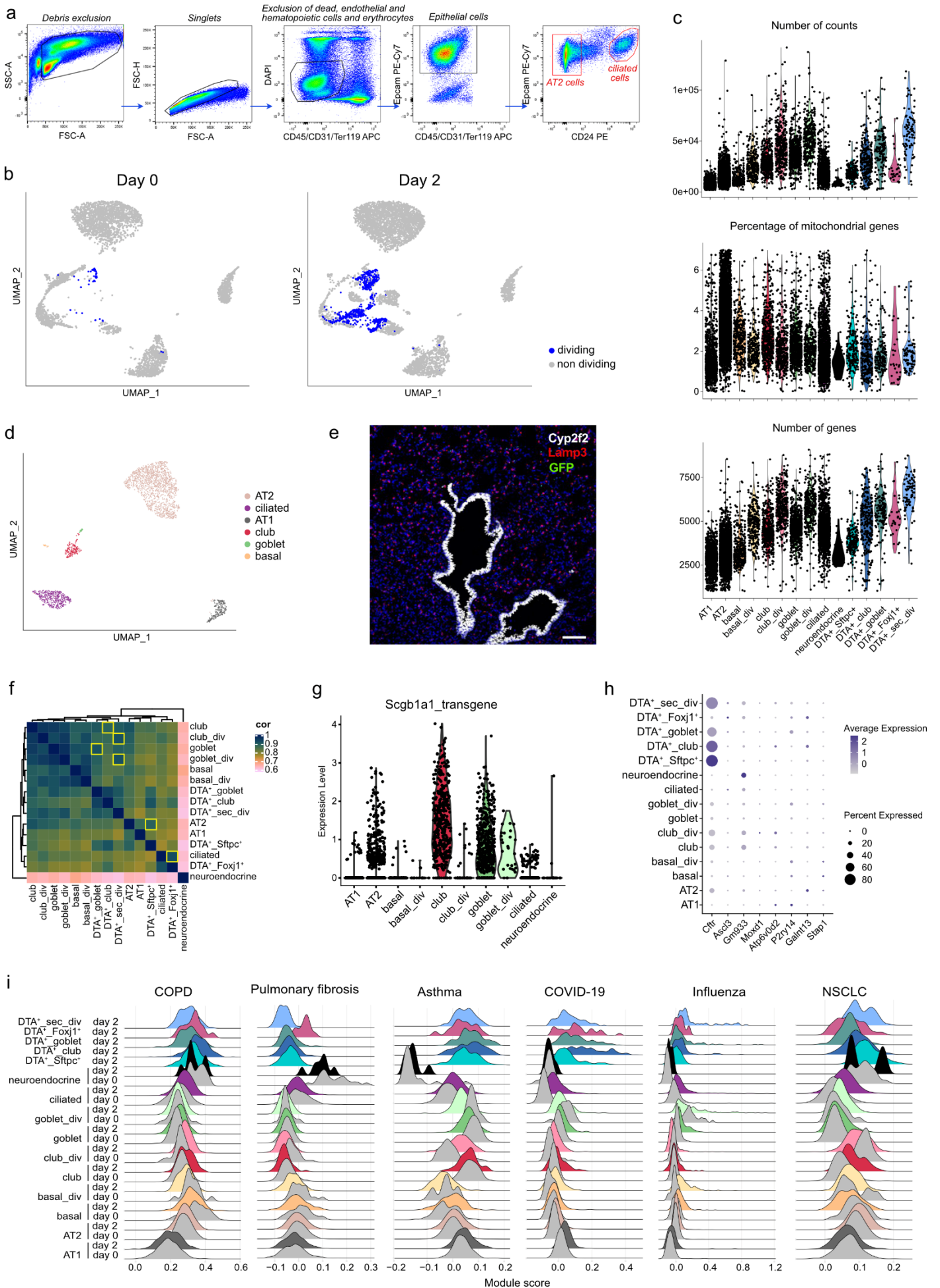


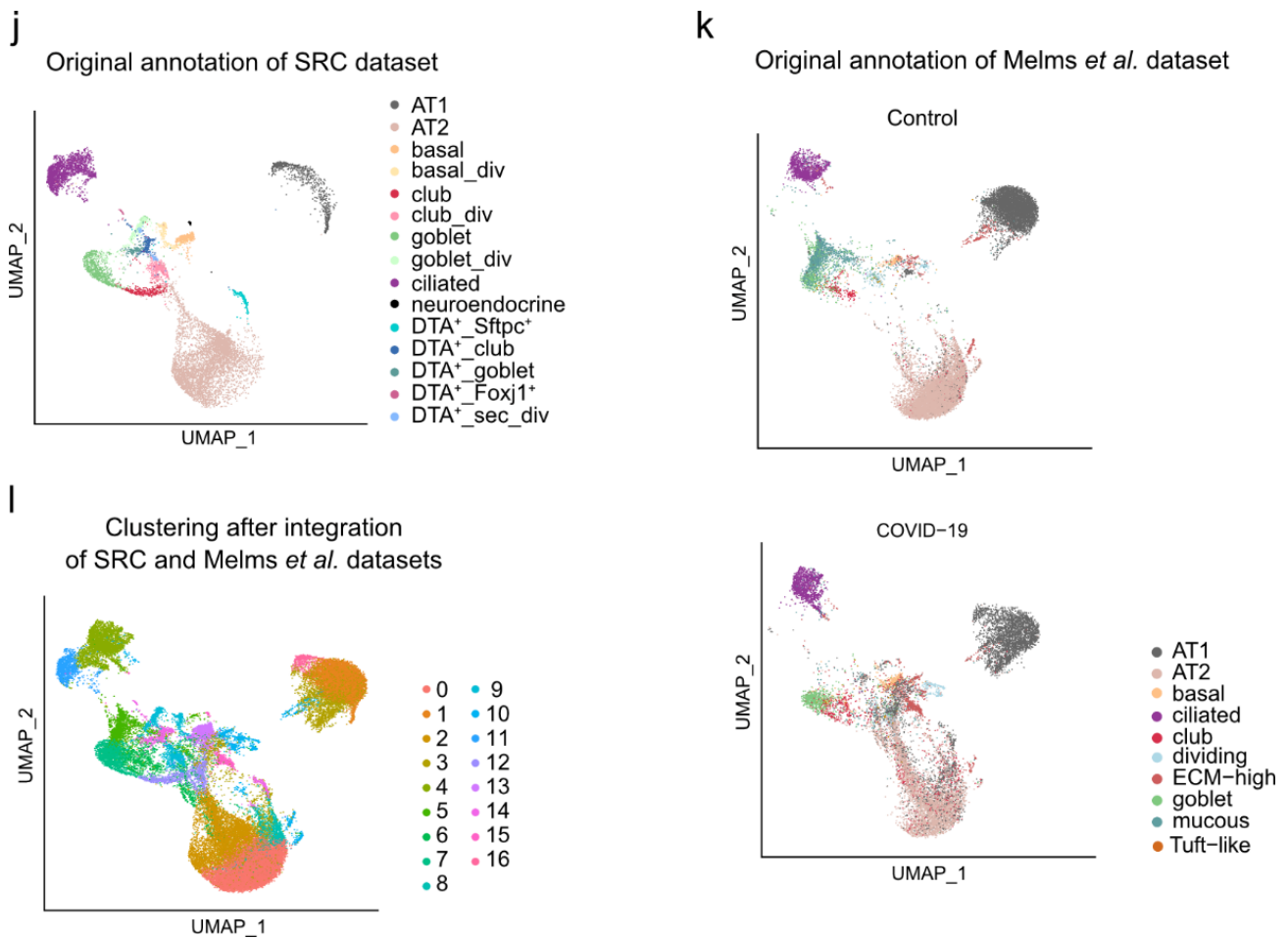


Supplementary Figure 3. Transcriptional changes in epithelial lung cells after *Scgb1a1*⁺ cell depletion.

a. Gating strategy used to sort epithelial cells, while keeping only 10% of AT2 cells (MHC II⁺) in relation to the total number of cells (red gate), and gating strategy to sort GFP⁺ epithelial cells. Percentage of GFP⁺ epithelial cells in relation to total epithelial cells on day 0 to 4 is indicated. **b.** IF staining of SRC mouse lungs with Cyp2f2 (white; club cells), CycB1-GFP (green; dividing cells), and DAPI (blue; nuclei) before (day 0) and 2, 3, and 4 days after injecting tamoxifen on two consecutive days. GFP⁺ spindle-like cells (arrows) and GFP⁺ alveolar cells (arrow heads) can be observed from day 3. Aw: airway. Scale bar: 100 μ m. Images are representative of at least three independent experiments with n=3 animals per timepoint. **c.** Dot plot showing the average scaled expression and the percentage of cells expressing cell type-specific marker genes across the epithelial populations. **d.** UMAP embedding (left) and violin plot (right) showing

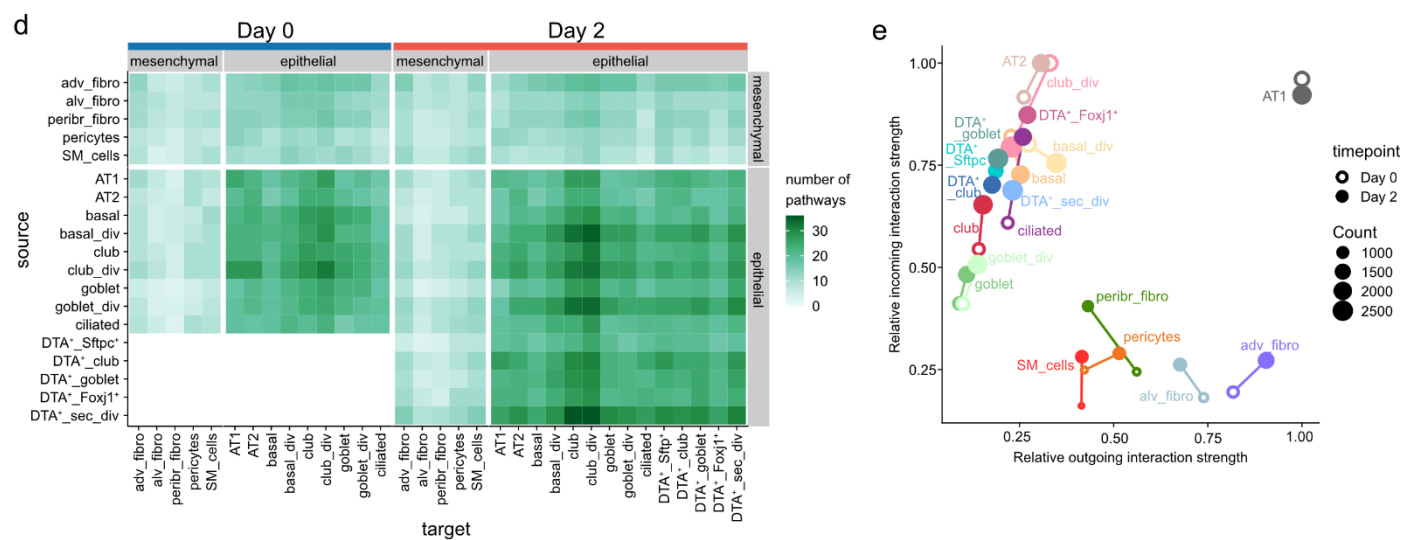
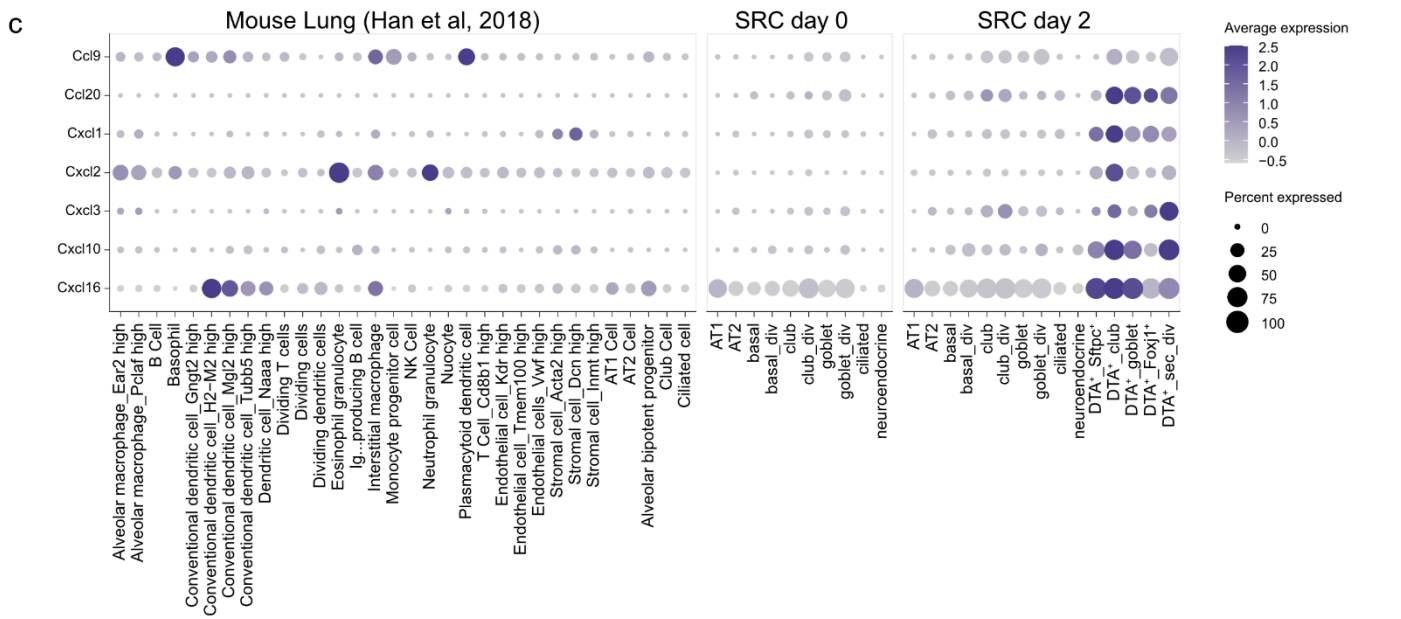
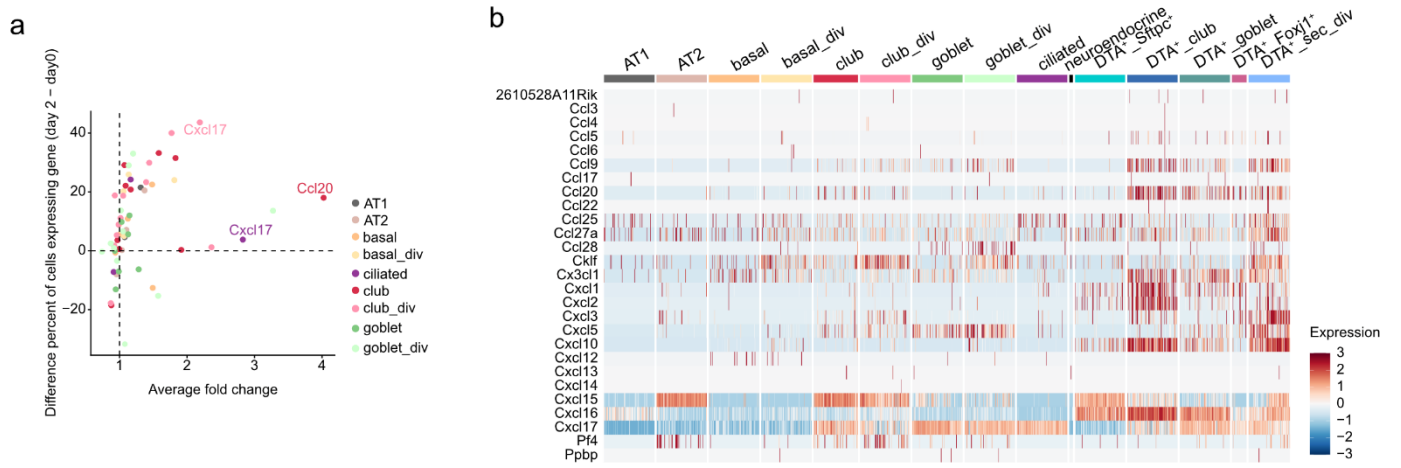
the expression of DTA in epithelial cell types from day 0 to day 4. **e.** GSEA of DEGs on day 2, 3, and 4 compared to day 0 (MAST test, $FC \geq 2$, $p_{adj} < 0.05$) in the different epithelial populations. **f.** Expression of DEGs in AT2 cells through time (MAST test, $FC > 2$, $p_{adj} < 0.05$). Genes in bold are mentioned in the text. Genes in red are related to cell division. **g.** Number of DEGs at the indicated days as compared to day 0 for all epithelial cell types (MAST test, $FC > 2$, $p_{adj} < 0.05$).

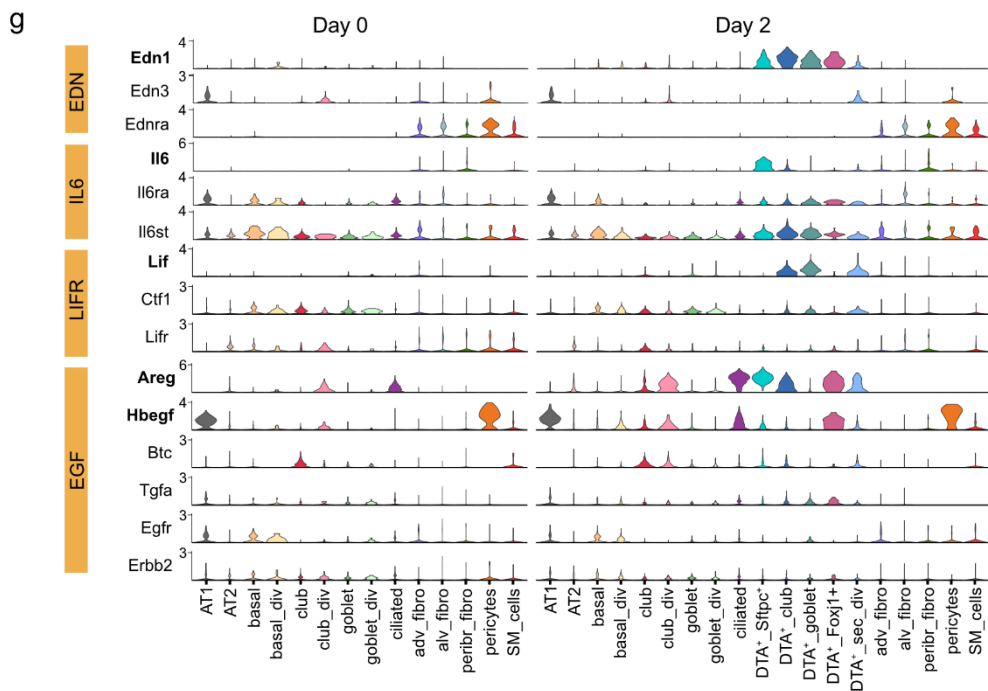
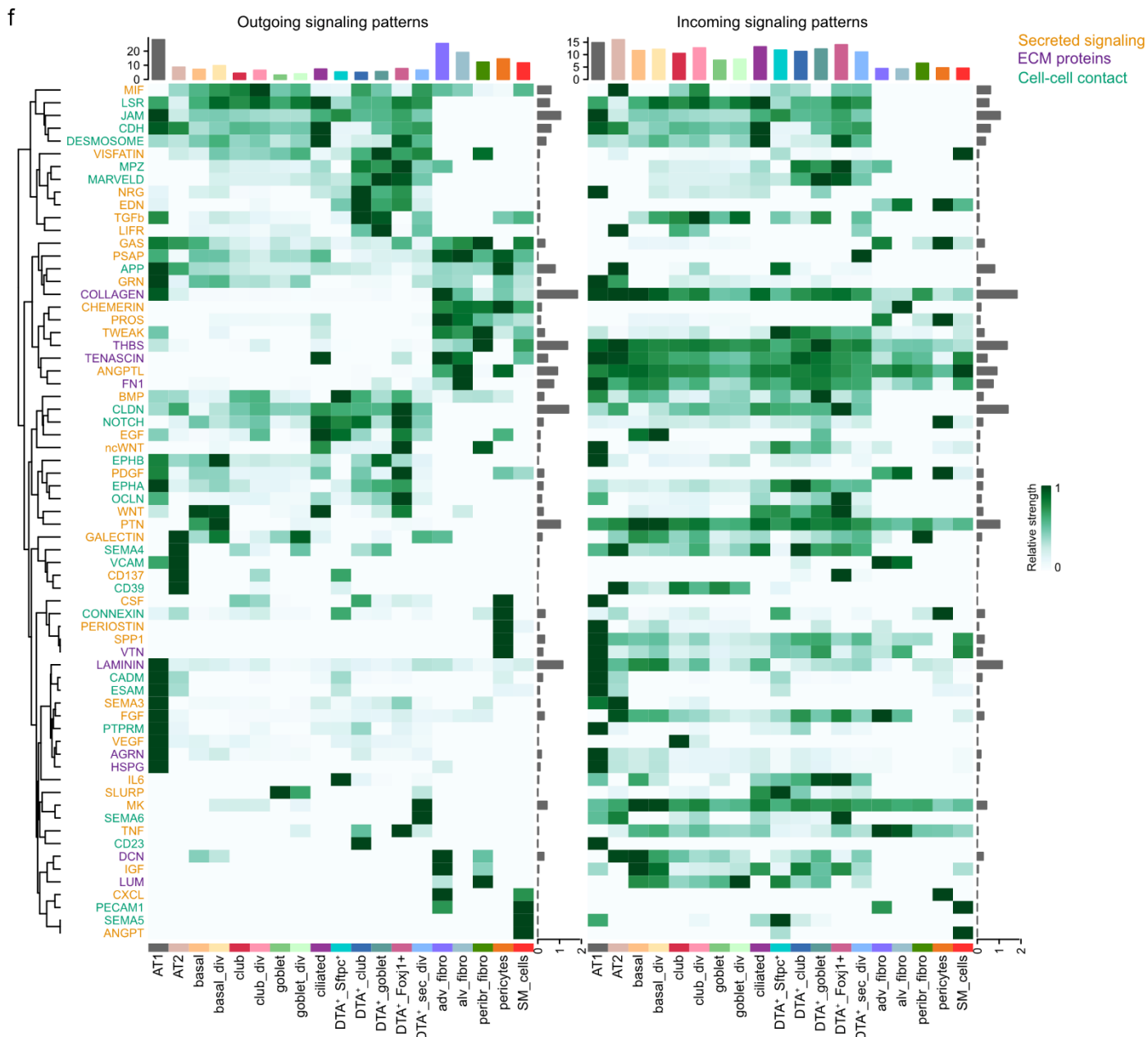




Supplementary Figure 4. Characterization of DTA⁺ epithelial cells and comparison to transcriptional profiles of human lung diseases.

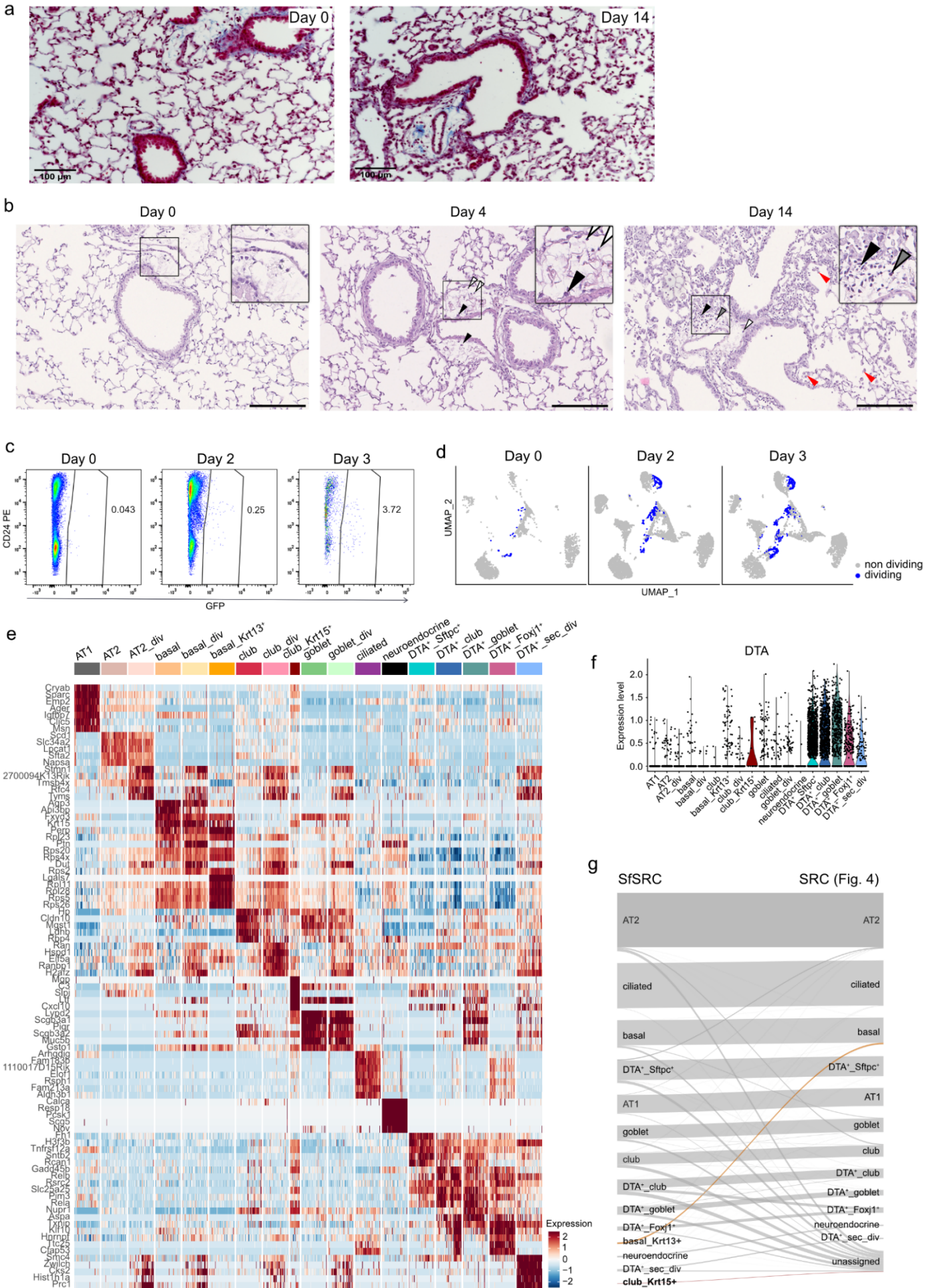
a. Gating strategy used to sort epithelial cells, while keeping only 10% of AT2 cells (CD24⁻) and 10% of ciliated cells (CD24^{high}) in relation to the total number of cells (red gates). **b.** UMAP embedding showing the distribution of dividing and non-dividing cells. **c.** Violin plots showing number of counts, percentage of mitochondrial genes, and number of genes in each cell types. The labeling of the y-axis is given in the heading. **d.** UMAP embedding showing epithelial cell types in Rosa26R-DTA x CycB1-GFP control mice (n=9) on day 2 after two consecutive tamoxifen injections. The sorting and sequencing strategy was the same as for SRC mice. **e.** IF staining of Rosa26R-DTA x CycB1-GFP control mouse lungs with Cyp2f2 (white; club cells), Lamp3 (red; AT2 cells), CycB1-GFP (green; dividing cells), and DAPI (blue; nuclei) on day 2 after injecting tamoxifen. Scale bar: 100 μ m. Images are representative of n=3 mice. **f.** Heatmap of the transcriptome Spearman correlation coefficient (cor) between all epithelial cell types on day 2. Yellow boxes highlight the closest population to each DTA⁺ cell type. **g.** Violin plot of the Scgb1a1 transgene expression on day 0 across all epithelial cells in SRC mice. **h.** Dot plot of ionocyte marker gene expression in all epithelial cell populations at day 2. **i.** Ridge plots showing the expression of human lung disease signatures in SRC mouse epithelial cells on day 0 and day 2. Gene signatures for asthma, non-small cell lung carcinoma, and influenza were taken from DisGeNET v7 ¹, and chronic obstructive pulmonary disease ², COVID-19 bronchial epithelial cells ³, and pulmonary fibrosis ⁴ from MSigDB v7.5.1 ^{5,6}. **j-i.** UMAP embedding after integration of SRC and Melms *et al.* ⁷ datasets showing the original annotation of cells from the SRC dataset (**j**), the original annotation of cells from the Melms *et al.* dataset (**k**), and re-clustering of both datasets (**l**).

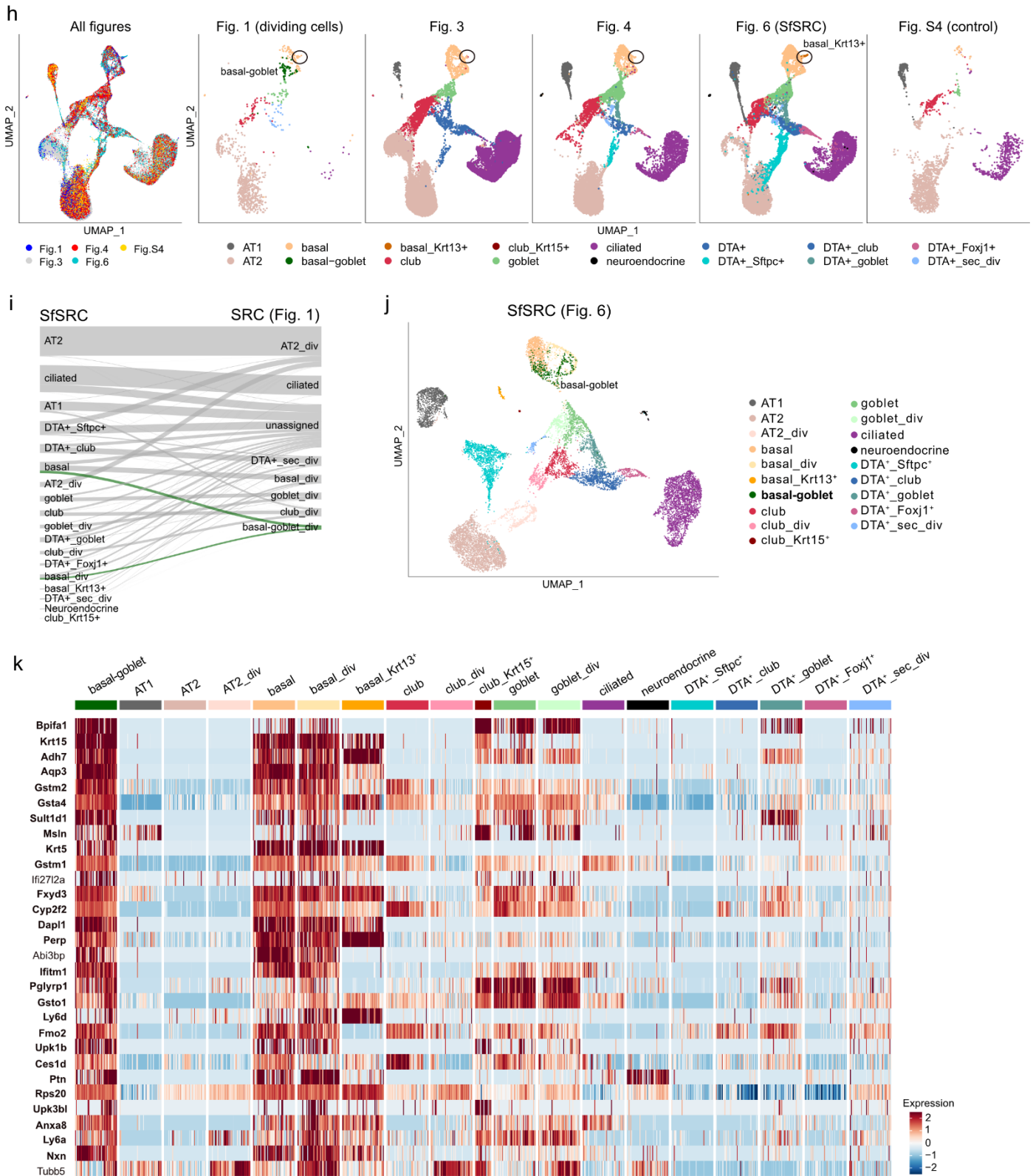




Supplementary Figure 5. Chemokine expression and cellular crosstalk in the SRC mouse model.

a. Differential expression of chemokines in epithelial lung cells upon injury. Only genes detected in at least 20% of cells in a population in either of the timepoints are shown. Genes with $FC > 2$ and $p_{adj} < 0.05$ are labeled (MAST test). **b.** Heatmap of chemokine expression in epithelial lung cells on day 2. Scaling of expression was done after downsampling to 100 cells per cell type. Chemokines without counts in any of the cell types were excluded. **c.** Dot plot showing the average scaled expression and the percentage of cells expressing selected chemokines (see Fig. 5b) in lung cells in homeostasis from the mouse atlas of Han *et al.*⁸ and in epithelial lung cells of the SRC model on day 0 and day 2. **d.** Number of signaling pathways between any two cell types before (day 0) and after tamoxifen administration (day 2) of the modified CellChat ligand-receptor database. **e.** Summed incoming and outgoing interaction strength of each cell type. The interaction strength was scaled to the maximum summed interaction strength at the respective timepoint. Circle size is proportional to the number of significant ligand-receptor pairs of the respective cell type at that timepoint. **f.** Heatmaps of outgoing (left) and incoming (right) signaling patterns per cell type on day 2. The signaling strengths are scaled to the maximum of each row. Column annotations show the summed absolute signaling strengths of each cell type. Row annotations show the log information flow (i.e. summed signaling strength) of each pathway. Signaling pathways are colored by the type of interaction (yellow: secreted signaling, purple: ECM proteins, green: cell-cell contact) and sorted according to the dendrogram of outgoing signaling patterns. **g.** Violin plots showing normalized expression of the main ligand and receptor genes contributing to the EDN, IL6, LIFR, and EGF signaling pathways on day 0 and day2.

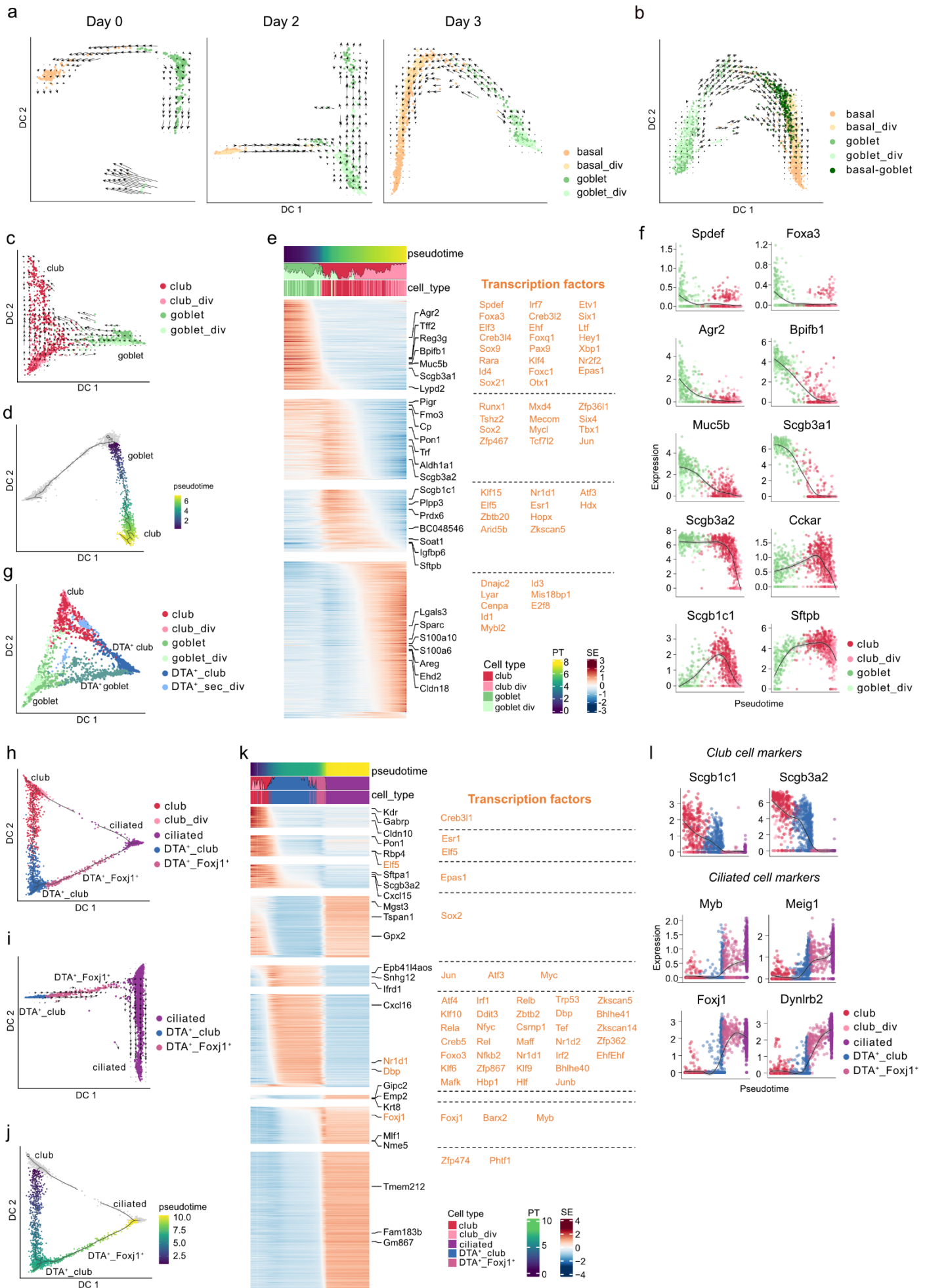




Supplementary Figure 6. Characterization of lung epithelial cells in the SfSRC mouse model.

a. Masson staining of SfSRC mouse lungs before (day 0) and 14 days after two consecutive tamoxifen injections. Images are representative of $n=3$ mice per timepoint and two independent experiments. Scale bar: 100 μm . **b.** H & E staining of SfSRC mouse lungs before (day 0), and 4 and 14 days after two consecutive tamoxifen injections. Images are representative of one experiment with $n=2$ mice per timepoint. Black arrowhead: plasma cell; white arrowhead: lymphocyte; gray arrowhead: neutrophil granulocyte; red arrowhead: alveolar macrophage. Scale bar: 200 μm . Insets on the top right on each picture are 2x magnifications of the demarcated area in the main picture. **c.** Flow cytometry plots showing the percentage of GFP⁺ epithelial cells in relation to total epithelial cells before (day 0) and two and three days after tamoxifen injection in SfSRC mouse lungs. **d.** UMAP embedding showing dividing and non-dividing cells on day 0, 2, and 3. **e.** Heatmap of the top five marker genes ranked by power across all epithelial populations (all three timepoints merged). **f.** Violin plot showing the expression of DTA in the indicated cell types (all three timepoints merged). **g.** Sankey diagram of SfSRC mouse epithelial cells projected onto SRC mouse epithelial cells using scmap. **h.** UMAP

embedding of all scRNA-seq datasets integrated (left), and the same UMAP showing the original cell type annotation in the different figures without discriminating cell cycle status. Circles depict the location of the basal_Krt13⁺ cell population. **i.** Sankey diagram of SfSRC mouse epithelial cells projected onto SRC mouse epithelial dividing cells using scmap. **j.** UMAP embedding of scRNA-seq data presented in Fig. 6 showing the distribution of basal-goblet cells (identified in **i**) in relation to other cell types. **k.** Heatmap of the top 30 upregulated genes in basal-goblet cells of the SfSRC model (identified in **i**) ranked by fold change (test= MAST, p_{adj} < 0.05). Genes in bold are common markers to basal-goblet_div cells from Fig. 1.



Supplementary Figure 7. Trajectory analysis of lung epithelial cells in the SfSRC mouse model.

a. Diffusion maps of basal and goblet cells with RNA velocity vectors calculated individually for each timepoint. **b.** Diffusion map of basal, goblet, and basal-goblet cells with RNA velocity vectors indicating transition from goblet to basal through basal-goblet cells. **c.** Diffusion map of goblet and club cells with RNA velocity vectors indicating differentiation of goblet into club cells. **d.** Diffusion map of basal, goblet, and club cells with pseudotime trajectory colored by pseudotime of cells selected to characterize the goblet to club cell trajectory in e. **e.** Smoothed expression heatmap of the top 1,000 altered genes along the differentiation trajectory from goblet to club cells. The names of the top seven genes in each cluster are annotated and transcription factors are marked in orange. All transcription factors of each cluster are listed on the right. **f.** Normalized expression along the goblet to club cell pseudotime trajectory for exemplary genes. The black line is the smoothed expression using local polynomial regression fitting, with the 95% confidence interval shown in gray. **g.** Diffusion map of all secretory cell types. **h.** Diffusion map of club, DTA⁺_club, DTA⁺_Foxj1⁺, and ciliated cells with pseudotime trajectory colored by cell type. **i.** Diffusion map of DTA⁺_club, DTA⁺_Foxj1⁺, and ciliated cells with RNA velocity vectors indicating transition of DTA⁺_club into DTA⁺_Foxj1⁺ cells. **j.** Diffusion map of club, DTA⁺_club, DTA⁺_Foxj1⁺, and ciliated cells colored by pseudotime of cells selected to characterize the club to ciliated cell trajectory in k. **k.** Smoothed expression heatmap of the top 1,000 altered genes along the differentiation trajectory from club to ciliated cells. The names of the top three genes in each cluster are annotated and transcription factors are marked in orange. All transcription factors of each cluster are listed on the right. **l.** Normalized expression along the club to ciliated cell pseudotime trajectory for exemplary genes. Smoothed expression and confidence interval are shown as in f. Figures were calculated on merged expression data of the SfSRC model from all timepoints (day 0, 2, and 3). PT: pseudotime; SE: scaled expression.

References

1. Pinero J, *et al.* The DisGeNET knowledge platform for disease genomics: 2019 update. *Nucleic Acids Res* **48**, D845-D855 (2020).
2. Ning W, *et al.* Comprehensive gene expression profiles reveal pathways related to the pathogenesis of chronic obstructive pulmonary disease. *Proc Natl Acad Sci U S A* **101**, 14895-14900 (2004).
3. Blanco-Melo D, *et al.* Imbalanced Host Response to SARS-CoV-2 Drives Development of COVID-19. *Cell* **181**, 1036-1045 e1039 (2020).
4. Kohler S, *et al.* The Human Phenotype Ontology in 2021. *Nucleic Acids Res* **49**, D1207-D1217 (2021).
5. Subramanian A, *et al.* Gene set enrichment analysis: a knowledge-based approach for interpreting genome-wide expression profiles. *Proc Natl Acad Sci U S A* **102**, 15545-15550 (2005).
6. Liberzon A, Birger C, Thorvaldsdottir H, Ghandi M, Mesirov JP, Tamayo P. The Molecular Signatures Database (MSigDB) hallmark gene set collection. *Cell Syst* **1**, 417-425 (2015).
7. Melms JC, *et al.* A molecular single-cell lung atlas of lethal COVID-19. *Nature* **595**, 114-119 (2021).
8. Han X, *et al.* Mapping the Mouse Cell Atlas by Microwell-Seq. *Cell* **172**, 1091-1107 e1017 (2018).